Risk Management of Airfield Obstacle Free Space Based on Supervised Neural Network

WU Peng[1], CHONG Xiao-lei[1], WANG Si-jia[2]

[1]Aeronautical Engineering College, Air Force Engineering University, Xi'an 710038, China, [2]Residential Environment and Construction Engineering College, Xi 'an Jiaotong University, Xi'an 710049, China

15131361026@163.com

Abstract. In the application of current airfield clearance standard, operation differences are neglected. As a result, this paper sets up a distributional pattern of flight paths at some airfield and new obstacle limitation standards on various security target levels. It interprets and fits the flight data into actual trajectory curves and applies BP neural network to build a prediction model of the spatial position of aircrafts. Based on this theory, the model is implemented in further statistical analyses of the original and simulation data collected in this airfield, which leads to the establishment of distribution rules of aircraft trajectory. This paper proposes a fresh method to set up an airfield obstacle free space and has important reference values to improve the administration of airfield obstacle free space.

1. Introduction

Airfield obstacle free space refers to the delimitation of a certain airspace near the airfield to protect safe transitions of aircraft. The height of buildings in this space is limited according to the obstacle free space regulation. The Civil Aeronautics Board proposes an obstacle removal solution according to flight procedures [1] while some researchers conduct obstacle free space assessment and obstruction management via geographic information system (GIS) [2-3]. Besides, International Civil Aviation Organization (ICAO) raises the concept of obstacle limitation surface [4] and a collision risk model is built to directly present airfield obstacle free space on the basis of probabilit[y] [5-6]. Yet, the delineation of obstacle free space still follows the old approach in "Airfield Clearance Specification" which sets the scope of airfield obstacle free space and limit obstacle height based on airfield level. In other words, airfields of the same level, though located in different regions, share the same requirements concerning the scope of obstacle free space and obstacle height limitation. Delineating clearance space in this way is not specific enough and can lead to unnecessary restrictions. This paper attempts to put forward an approach to delineate airfield obstacle free space by running statistics of the operation trajectory of resident aircrafts so as to improve the precision of airfield obstacle free space.

2. Acquisition of aircraft operating data

2.1. The Principles of data interpretation

In order to describe the attitude of the aircraft flight accurately, the body coordinate system is established. The angle between the X axis, which is along the longitudinal axis of the aircraft, and the horizontal line is the pitch angle θ; the angle between the forward direction of the wing and the wing

Content from this work may be used under the terms of the Creative Commons Attribution 3.0 licence. Any further distribution of this work must maintain attribution to the author(s) and the title of the work, journal citation and DOI.
Published under licence by IOP Publishing Ltd

chord is the angle of attack α; the angle between the X axis and the North Pole of the Earth is the heading angle ψ, and so forth.

These angle data as well as the real-time speed data of aircrafts are recorded in the flight data recorder. After the velocity V, refers to the velocity in vacuum, is decomposed into three velocities on X, Y, Z directions by angular relationship, the aircraft displacement of a very short time towards all directions is generated. Use the velocity integral method to obtain the accumulation of displacement relative to the initial position at a certain moment, which can be recognised as space coordinates. At this moment the coordinate origin is regarded as the starting point for the aircraft. The X axis takes the moving direction of the aircraft along the middle line of the runway as positive while the Y axis is perpendicular to the middle line of the runway. the Z axis is perpendicular to the XOY plane and the coordinates in X, Y and Z directions are obtained by the Equation 1:

$$X_i = \sum_{j=0}^{i} V \cdot \Delta t \cdot \cos(\vartheta - \alpha)\cos(\psi - \beta)$$

$$Y_i = \sum_{j=0}^{i} V \times \Delta t \times \cos(\vartheta - \alpha)\sin(\psi - \beta)$$

$$Z_i = \sum_{j=0}^{i} V \cdot \Delta t \cdot \sin(\vartheta - \alpha); i = 0,1,\cdots,n \quad (1)$$

In the aforesaid equations, β is the angle between the runway and the true north direction, i is the number of flight parameters. Then the X axis should be converted to the airport coordinate with the origin at the middle of finish line.

2.2. Calculation and fitting of aircraft operation data

Considering the continuous changes of aircraft attitude in the air, the missing data in the corresponding flight moment can be obtained by applying cubic spline interpolation on adjacent data. With the equations above, the trajectory of aircrafts recorded by flight parameters recorder can be obtained. Figure 1(a) is a flight path in take-off stage generated through the speed integral method. Figure 1(b) shows the distribution of aircraft positions of 22 flights obtained through velocity integral method.

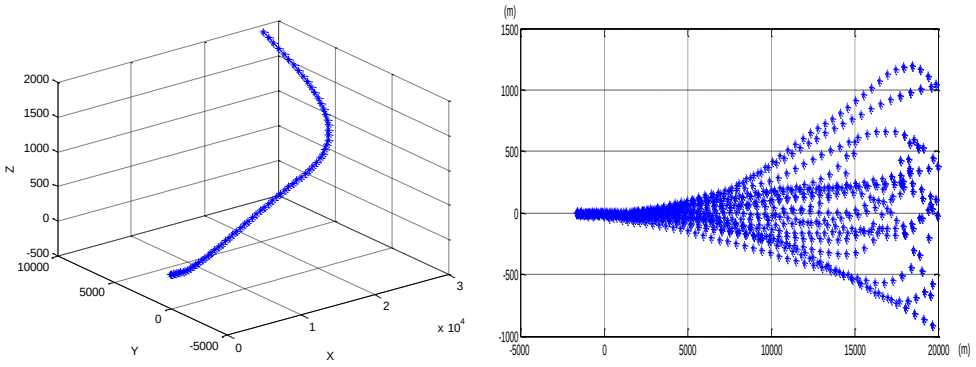

(a) (b)

Fig 1. Flight path sketch.

In Figure 1(b), the value of X coordinate ranges from -1700 to 20,000, that is, from the position where the aircraft starts to run to the boundary of the obstacle free space. The coordinates fitting of X and Z images are shown in Figure 2.

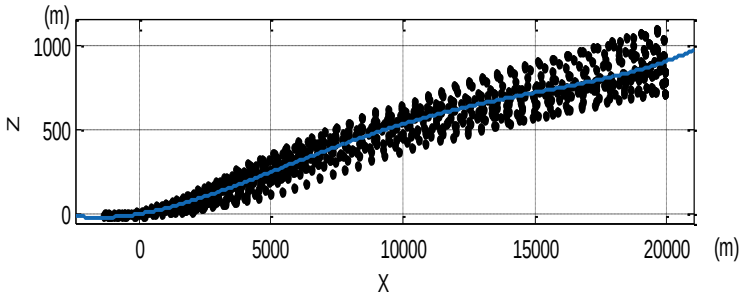

Fig 2. Movement and fitting situation of XOZ plane.

With the above method, it can be concluded that the operation trajectory of a certain model of aircraft at a specific airfield is a comprehensive result that is caused by various factors such as weather, altitude and driving, and is in line with the actual operation of the airfield.

3. Statistics and analysis of aircraft operational laws

The next step is to perform statistical analysis on a large amount of data to reveal the distribution of aircraft trajectories. However, because of various restrictions, the operating parameters of aircrafts are always limited under specific conditions. In order to expand the statistical data and increase the reliability of statistical results, this paper uses the neural network method to simulate the position coordinates of aircraft based on existing data.

3.1. Construction of supervised neural networks

Supervised neural network is a multi-layer feed-forward network trained by the algorithm of backward propagation of errors[7]. The learning process includes two phases: forward propagation of signals and backward propagation of errors. It can advance the training process with real-time correction of errors and minimise the SSE of the network through a constant adjustment of the weights and enthalpies. In the construction of a supervised neural network, *i* refers to the number of input layer neurons, *j* hidden layer neurons, and *k* output layer neurons. The output is as follows:

$$z^1 = \text{tansig}(IU^{1,1}x^1 + y^1) \tag{2}$$

$$B = z^2 = \text{purelin}(LU^{2,1}z^1 + y^2) \tag{3}$$

Where, x is the input vector, IU1,1 and LU2,1 are the weight vectors, y is the offset, z is the intermediate variable, B is the output, tansig, purelin are the transfer functions used by the hidden layer and the output layer, respectively.

3.2. Analysis of training results

Although supervised neural network is widely used in information, automation and other fields, it is still necessary to optimize the solutions in a more targeted way by combining experience with actual conditions to solve the problem of this paper. In the actual simulation, this is realised by adjusting the number of neurons in the hidden layer j and the radial basis spreading rate *spread*.

Take the training results of X and Z coordinates as an example. In Figure 3, on the left side is an aircraft motion image generated from measured flight data in the XOZ plane, while the right one is generated from training. The trends are basically identical.

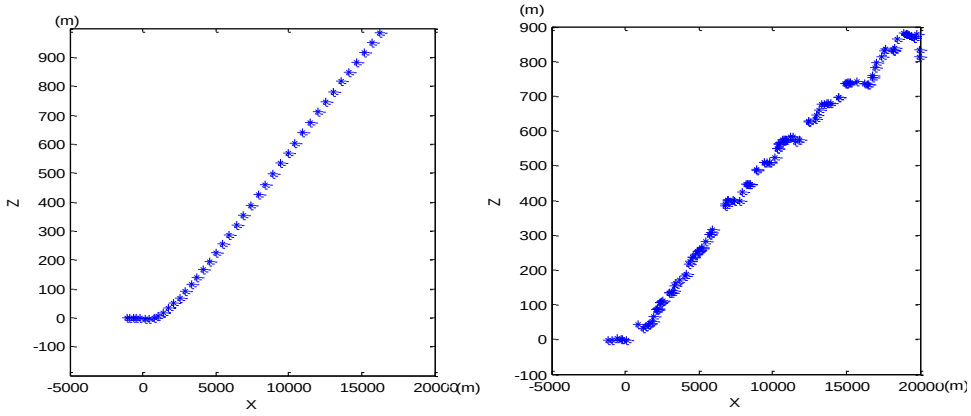

Fig 3. Prediction of movement in XOZ plane.

Figure 4 (a) is the comparison of the training results of BP and RBF networks, two kinds of typical supervised neural network, which shows that the former is better. Figure 4 (b) shows the regression analysis, in terms of the value of the correlation coefficient R corresponding to the regression of training set, validation set, test set, and overall regression. The R values of the four parts are all close to one, and the four fitting curves are located in the diagonal positions of their images respectively, indicating a good training condition.

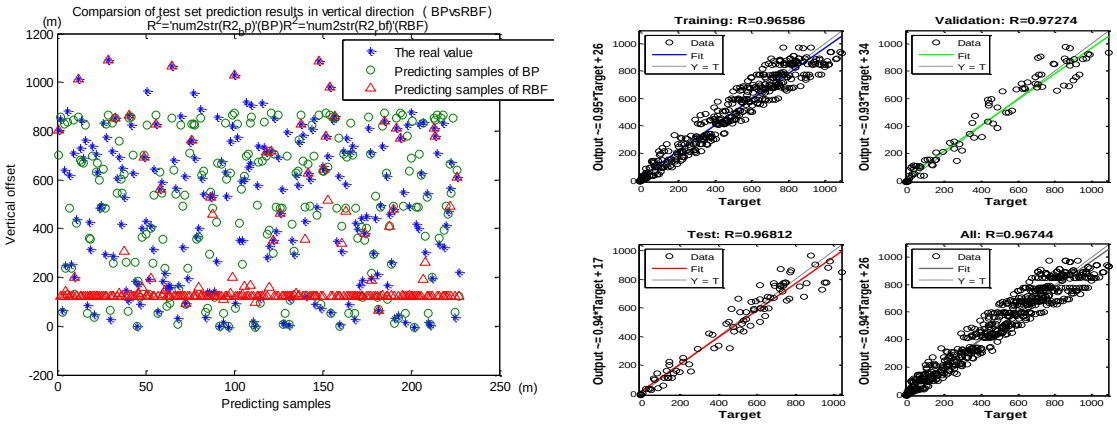

(a) (b)

Fig 4. Analysis of Training Results.

Due to the small volume of the original data, this paper adopts BP and RBF neural networks to train data and perform comparative analysis so as to determine the value of the Z coordinate corresponding to any X coordinate by their intrinsic correspondence. It makes the analysis and expansion of flight data via BP neural network become possible.

4. The distribution rules of aircraft in obstacle-free space and its setting

Using the method established above, this paper collects 68 flight records in some airfield, runs calculation with the speed integration method and simulation with BP neural network and as a result obtains the distribution of aircraft trajectories in the terminal obstacle free space. It then analyses the scope of the obstacle free space.

4.1. Distribution analysis and parameter estimation

When X ranges from 0 to 20000, take 200 m as a section and calculates the distribution of Z values. The typical distribution histograms are as follows:

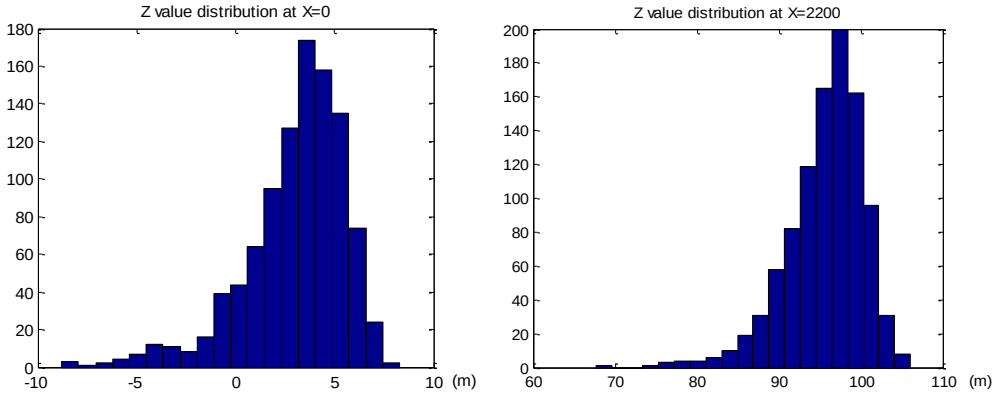

Fig 5. Distribution of Z for different X.

Based on the analysis of Figure 5 and the actual situation in flight, assume the longitudinal offset conforms to an extreme type I distribution, the distribution equation is:

$$\mathrm{F}(x,a,b)=\exp\{-\exp(-\frac{(x-b)}{a})\},-\infty<x<+\infty \tag{4}$$

Use the maximum-likelihood method [8]to estimate the parameters a, b of the I-type extreme value distribution. First, construct a general likelihood function of the extreme value distribution:

$$\mathrm{L}(\mathrm{a},b)=\prod_{i=1}^{n}\frac{dF(x)}{dx}=\left(\frac{1}{a}\right)^{n}\prod_{i=1}^{n}\left(1+\varepsilon\cdot\frac{x_i-b}{a}\right)^{\frac{\varepsilon+1}{\varepsilon}}\cdot\exp\left\{-\sum_{i=1}^{n}\left(1+\varepsilon\cdot\frac{x_i-b}{a}\right)^{-\frac{1}{\varepsilon}}\right\} \tag{5}$$

According to the maximum-likelihood method, set:

$$\frac{\partial L(a,b)}{\partial a}=0,\frac{\partial L(a,b)}{\partial b}=0. \tag{6}$$

In the I-type extreme value distribution:

$$\sum_{i=1}^{\mathrm{n}}x_i\exp\left(-\frac{x_i}{\hat{a}}\right)-(\bar{x}-\hat{a})\cdot\sum_{i=1}^{\mathrm{n}}x_i\exp\left(-\frac{x_i}{\hat{a}}\right)=0 \tag{7}$$

$$\hat{\mathrm{b}}=-\hat{a}\cdot\ln\left[\frac{1}{n}\cdot\sum_{i=1}^{\mathrm{n}}x_i\cdot\exp\left(-\frac{x_i}{\hat{a}}\right)\right] \tag{8}$$

4.2. Distribution test method

Assume that the longitudinal deviation agrees with the extreme I-type distribution and estimate its parameters, then adopt the Lilliefors test for verification[9]. The basic principle is:

(1) Hypothesis H_0: the empirical distribution function Sn (X) of standardized samples follows the theoretical cumulative distribution function φ (X).

(2) Rearrange subsamples according to their values from the smallest to the largest, denote as X_i.

(3) Determine the maximum deviation D_n of the empirical distribution function from the theoretical cumulative distribution function.

$$D_n = \sup_{-\infty<x<+\infty} \left|S_n(x) - \varphi(x)\right| = \max_{1\le i\le n} \delta_i \tag{9}$$

(4) The given significant level α, look up the maximum allowable deviation $D_{n,a}$ of the critical value table of the Lilliefors test. If $D_{n,a} > D_n$, accept hypothesis H_0. Otherwise, reject hypothesis H_0 for it indicates the distribution function of the sample does not conform to this distribution type. Therefore, the distribution function must be assumed separately.

4.3. Statistics of aircraft altitude in obstacle-free space

The mean values $\overline{Z}$, standard deviations σ_z of the Z coordinates corresponding to different X coordinates, the extreme value distribution parameters $\hat{\alpha}, \hat{b}$ corresponding to the Z coordinate array, and the values under different confidence values corresponding to the test results and Z coordinates are shown in Table 1.

Table 1. Statistics of Z for different X.

X	$\overline{Z}$	σ_Z	$\hat{b}$	$\hat{a}$	H_0	Z values under different confidence values		
						α = 0.05	α = 0.01	$\alpha = 5\times10^{-9}$①
1000	35.58	5.63	4.15	38.14	1	31.80	33.58	25.89
1600	66.18	5.58	4.17	68.67	1	62.30	64.10	56.37
2200	95.49	4.89	3.77	97.65	1	91.90	93.52	86.54
2800	123.94	5.81	4.66	126.51	1	119.39	121.40	112.76
3400	156.46	6.80	5.47	159.52	1	151.17	153.52	143.39
4000	194.54	9.60	7.60	199.07	1	187.46	190.73	176.64
4600	227.36	10.68	8.32	232.21	1	219.51	223.08	207.67
5200	271.11	10.83	9.19	276.19	1	262.16	266.11	249.08
5800	306.26	12.98	10.11	312.11	1	296.67	301.01	282.28
6400	340.57	14.65	11.25	346.87	1	329.69	334.52	313.67

Note: $\alpha = 5\times10^{-9}$ is the ICAO safety standard adopted for Civil Aviation of China[10].

4.4. Statistics-based settings of obstacle free space

Confidence intervals in Table 1 reflect the possibility of an aircraft appearing in a certain height range. It can be considered as a different safety target which can be adjusted according to actual demands and can be used to calculate the corresponding height range. The height limitation is shown in Figure 6(a) where safety targets correspond to the three curves. In theory, the closer the obstacle is to the limit curve, the higher the risk coefficient is, that is, the area has a lighter to darker gradient. Figure 6(b) is the corresponding plane range:

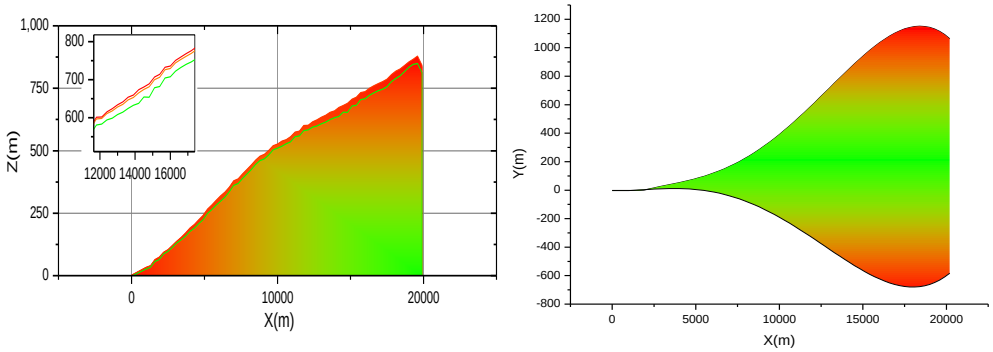

(a) (b)

Fig 6. Map of airport clearance in XOZ and XOY.

Combine the plane range with the height limitation to generate the limitation criteria of obstacle free space for different safety goals of the airfield, as shown in the following figure:

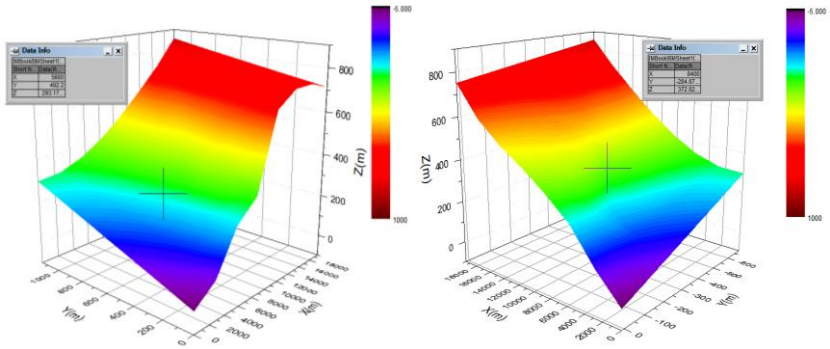

Fig 7. Clearance limited plane when $\alpha = 10^{-9}$.

The standard maps above can also be used for querying, that is, through the surface, the height limit of obstacles corresponding to different safety targets can be determined at any point in the airfield coordinate system. Similarly, it is possible to set obstacle limitations for specific airfield and manage obstacle in the terminal obstacle free space with the ideas and methods set forth in this paper.

5. Conclusion

This paper adopts velocity integral method to analyse airborne flight parameters. Based on the acquired spatial position data of aircrafts, BP neural network is used to construct the prediction model of aircraft spatial position. After processing the flight parameters of some airfield, it provides obstacle limitation standards under different security objectives. This paper presents a method for delineating the obstacle-free space built on the characteristics of aircraft operation in airfield from the aspects of data acquisition, simulation analysis, data statistics and delineation of obstacle-free space, as well as a new perspective for managing airfield obstacle-free space.

References

[1] Civil Aeronautics Board，Technical standards for civil airport flight area.（MH5001-2013）[S].

[2] CHONG Xiaolei, XU Jinliang, CAI Liangcai. On the methods of obstructions management based on security in the airport clearance area [J]. Journal of Safety and Environment,2009, (1).

[3] LUO C L, CAI L C, et al. Assessment of military airfield obstacle free space based on GIS[J]. Transactions of Nanjing University of Aeronautics & Astronautics,2011, (3).

[4] International Civil Aviation Organization. Annex 14 to the Convention of International Civil Aviation-Aerodromes, Sixth Edition, Volume I-Aerodrome Design and Operations[s]. ICAO, 2013.

[5] International Civil Aviation Organization（ICAO）.Doc.9274-AN/904,Manual on the Use of the Collision Risk Model（CRM）for ILS Operations[S].1980.

[6] WU PENG, CHONG Xiaolei, GENG Hao. Evaluation Method of Clearance Obstacles Based on the Prediction Model of Aircraft Position[J]. Journal of Air Force Engineering University (natural science edition), 2018, 19(4):20-25.

[7] ZHU Daqi, SHEN Hui. Principle and application of artificial neural network[M].Sciences Press，2016.

[8] LU Anping; ZHAO Lin; GUO Zengwei; GE Yaojun. A comparative study of extreme value distribution and parameter estimation based on the Monte Carlo method[J]. Journal of Harbin Institute of Technology, 2013(2).

[9] ZHANG Gangyong; RUAN Luning. Comparison of several normal test methods based on

Monte Carlo simulation[J]. Statistics and Decision Making, 2011(7).
[10] Dong-bin Li, Xiao-hao Xu, Xiong-Li. Target level safety for Chinese airspace[J]. Safety Science, 47(2009)421-424.